Desalination and Water Treatment
www.deswater.com

28 (2011) 247–254
April

1944-3994/1944-3986
doi: 10/5004/dwt.2011.1853

Photodegradation study of congo red, methyl orange, methyl red and methylene blue under simulated solar irradiation catalyzed by ZnS/CdS nanocomposite

H.R. Pouretedal[a,*], S. Sabzevari[b]

[a]*Faculty of Science, Malek-Ashtsru University of Technology, Shahin-Shahr, Iran*
Tel. +98 312 5912253; email: hr_pouretedal@mut-es.ac.ir
[b]*Department of Chemistry, Islamic Azad University, Shahreza Branch, Iran*

Received 14 February 2010; Accepted 8 January 2011

ABSTRACT

The nanocomposites of $Zn_XCd_{1-X}S$ were synthesized via controlled co-precipitation. The X-ray diffraction pattern, transmission electron microscopy image and BET method were used to characterize the synthesized nanocomposites. The cubic structure of nanocomposites were confirmed using X-ray diffraction pattern. The photodegradation of congo red, methyl orange, methyl red and methylene blue catalyzed by prepared nanocomposites was studied under simulated solar irradiation. The $Zn_{0.4}Cd_{0.6}S$ show the highest photoactivity among nanocomposites. The effect of samples pH and $Zn_{0.4}Cd_{0.6}S$ dosage were adjusted to optimize the photodegradation process of dyes. The degradation efficiency of 95% were obtained within 20 min for congo red and 60 min for other dyes with initial concentration of 10 mg/l. The $Zn_{0.4}Cd_{0.6}S$ indicate the stability in samples with pH of 3–11. The mineralization of dyes was confirmed using determination of chemical oxygen demand of solutions after photodegradation process.

Keywords: Dye; Degradation; ZnS; CdS; Composite; Photocatalyst

1. Introduction

It is essential to synthesize the nanocomposites in order to manipulate the photocatalytic activity and enhance the functionality of semiconductor nanostructure. The band-gap is one of the factors that can influence on the photocatalytic activity of semiconductor nanocomposites. Therefore, the synthesis of nanostructures with different compositions is one of the attractive research fields in recent years [1,2]. The band-gap and hence of the photocatalytic activity of $Zn_XCd_{1-X}S$ nanocomposite changes with the composition. This nanostructure can produce hydrogen gas under visible light irradiation and also promising materials for high-density optical recording and short wavelength laser diode applications [3,4]. The thin films of this composition with wide band-gap have abroad application in devices such as solar cells and photodetectors [5–7]. Microemulsion, hydrothermal and precipitation methods were used to synthesis of $Zn_XCd_{1-X}S$ nanocomposites [3,8,9].

Dyes and pigments show one of the problematic groups in environment. They are arrived into waste waters from various industrial such as dye manufacturing and textile finishing and also from food coloring, cosmetics, paper and carpet industries [10,11]. About 1–20% of the total world production of dyes is lost during the dyeing process and released in the textile effluents. It is well known that some azo dyes and their degradation products such as aromatic amines are highly carcinogenic [12–14]. Among the various methods for removal of the textile dyes from wastewater such as adsorption, biodegradation, chlorination and

*Corresponding author.

ozonation, photodegradation is found as an emerging technology. The total mineralization of most of organic pollutants is the significant advantage of this method [15,16]. The use of semiconductors such as TiO_2, ZnS, ZnO, CdS, Fe_2O_3 and so on in photodegradation process as photocatalyst is one serious technique for increasing the rate of destruction. The high photocatalytic activity, resistance to photocorrosion, low cost, non-toxicity and favorable band-gap energy are the advantages of a worthy suitable photocatalyst. Thus, synthesis of different photocatalysts with various compositions and study of organic pollutants destruction can be an attractive field of researches [17,18].

In this article, we report the synthesis and characterization of $Zn_XCd_{1-X}S$ nanostructure particles. Also, photodegradation of congo red (CR), methyl orange (MO), methyl red (MR) and methylene blue (MB) catalyzed by prepared nanoparticles was presented in this article.

2. Experimental

2.1. Synthesis and characterization of nanocomposits

The nitrate salts of zinc and cadmium and sodium sulfide as precursor were used to prepare the $Zn_XCd_{1-X}S$ nanoparticles. The major chemicals were of reagent grade with highest purity and double distilled water was used to prepare solutions. 50 ml of 0.1 M Na_2S solution in a decanter vessel was added drop by drop into 50 ml of 0.1 M zinc and cadmium ions solution while the mixture was stirred vigorously at room temperature. The precursor solution is contain *X* ml 0.1 M of zinc nitrate and 50–*X* ml 0.1 M of cadmium nitrate. The *X* values are 50, 45, 40, 35, 30, 25, 20, 15, 10, 5 and 0. Thus, the $Zn_XCd_{1-X}S$ nanocomposits with *X* values 1, 0.9, 0.8, 0.7, 0.6, 0.5, 0.4, 0.3, 0.2, 0.1 and 0 were obtained as precipitated particles. The particles were separated, washed with deionized water and ethanol several times and dried in an oven at 80°C for 4 h.

The real content of Zn^{2+} and Cd^{2+} ions in $Zn_XCd_{1-X}S$ was determined using atomic absorption spectroscopy (AAS) method by using AA-6200 Shimadzu. A 0.2 g sample dissolves in least amount of nitric acid 2.0 M and the obtained solution dilutes in a volumetric flask of 50.0 ml. The absorbance of standard and sample solutions of zinc and cadmium ions was measured at wavelengths of 213.8 and 228.8 nm, respectively. A diffractometer Bruker D8ADVANCE Germany with Cu anode (λ = 1.5406 Å) and Ni filter was applied to record the XRD patterns of nanocomposits. The morphology and grain size of nanocomposits were observed by a JEOL JEM–1200EXII transmission electron microscope (TEM) operating at 120 kV.

2.2. Photodegradation of dye pollutants

The photodegradation of CR, MO, MR and MB catalyzed by $Zn_XCd_{1-X}S$ nanoparticles was performed in a Pyrex reactor at 25°C. The structure of dyes is shown in Fig. 1.

A 1000 W xenon lamp equipped with a cutoff filter of 350 nm was used as source irradiation. The reactor was filled with 50 ml of 5.0–50.0 mg/l of dye sample and 0.1–1.0 g/l of nanocomposite. The absorbance of samples before and after photodegradation at λ_{max} of dyes was used to determine the degradation efficiency. The absorbance of samples was measured by a UV–Vis spectrophotometer Carry-100 using a paired 1.0 cm quartz cell. The Millipore membrane filters and centrifuge of samples were used to remove the particles.

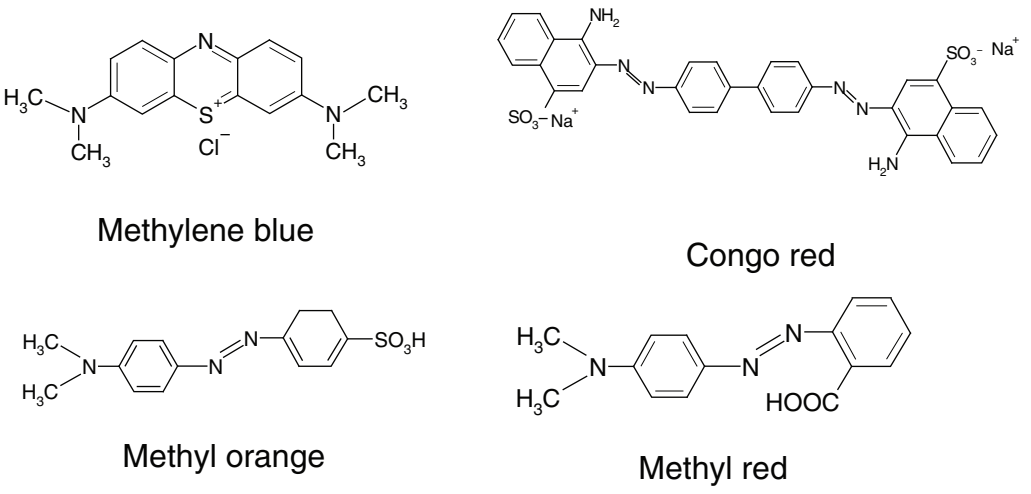

Fig. 1. The structure of dyes.

The rate of decolorization was estimated from residual concentration of dye by spectrophotometric method and degradation efficiency was calculated by Eq. (1)

$$\%\text{Degradation} = 100 \times [1 - (C_t/C_o)] \quad (1)$$

where C_0 and C_t are dye concentration at initial and time t, respectively.

Chemical oxygen demand (COD) was measured by the dichromate reflux method. The stability of $Zn_{0.4}Cd_{0.6}S$ nanocomposite was studied by subjecting the irradiated solutions to AAS analysis. The concentrations of Zn^{2+} and Cd^{2+} in solution resulting from dissolution or photocorrosion were determined.

3. Results and discussion

3.1. Characterization of $Zn_XCd_{1-X}S$ nanocomposite

The composition of nanocomposites was characterized by determination of zinc and cadmium ions using AAS method. The mole fractions of zinc and cadmium in prepared composites are given in Table 1. The obtained results confirm the formation of composites.

It has been reported that ZnS and CdS may have either cubic or hexagonal structure, depending on the synthesis conditions such as synthesis temperature and precursor concentration. The XRD patterns show the cubic structure for all of $Zn_XCd_{1-X}S$ nanocomposites. As a sample, the XRD pattern of $Zn_{0.4}Cd_{0.6}S$ was shown in Fig. 2. The existence peaks at 2θ of 28.7°, 47.5° and 56.1° correspond to the (1 1 1), (2 2 0) and (3 1 1) planes of the cubic phase of nanocomposite, respectively [19]. The $Zn_XCd_{1-X}S$ nanocomposite is a solid solution. The values in electronegativity of Cd (1.69) and Zn (1.65) are very close, which is favorable to form a solid solution alloy [3].

The crystalline sizes of the prepared nanoparticles are estimated from the Scherrer equation [20] that is indicated by Eq. (2)

$$D = \frac{0.9\lambda}{\beta \cos\theta} \quad (2)$$

where D is the crystalline size, λ is the wavelength of the incident X-ray (0.15406 nm), θ is the diffraction angle of the (1 1 1) peak of the cubic phase, and β is the half-width. The size of $Zn_{0.4}Cd_{0.6}S$ particles was obtained 5.7 nm accordance to the Scherrer equation. Transmission electron microscopy (TEM) images of $Zn_{0.4}Cd_{0.6}S$ nanocomposite is shown in Fig. 3. The particles size less than 50 nm were confirmed with respect to the TEM image. The specific surface area of $Zn_{0.4}Cd_{0.6}S$ nanocomposite was obtained 145 m^2/g by using BET method [21].

Table 1
The mole fractions of zinc and cadmium in composites

Composite	X_{Zn}	X_{Cd}
$Zn_{0.1}Cd_{0.9}S$	0.08	0.92
$Zn_{0.2}Cd_{0.8}S$	0.19	0.81
$Zn_{0.3}Cd_{0.7}S$	0.32	0.68
$Zn_{0.4}Cd_{0.6}S$	0.43	0.57
$Zn_{0.5}Cd_{0.5}S$	0.48	0.52
$Zn_{0.6}Cd_{0.4}S$	0.58	0.42
$Zn_{0.7}Cd_{0.3}S$	0.67	0.33
$Zn_{0.8}Cd_{0.2}S$	0.82	0.28
$Zn_{0.9}Cd_{0.1}S$	0.91	0.09

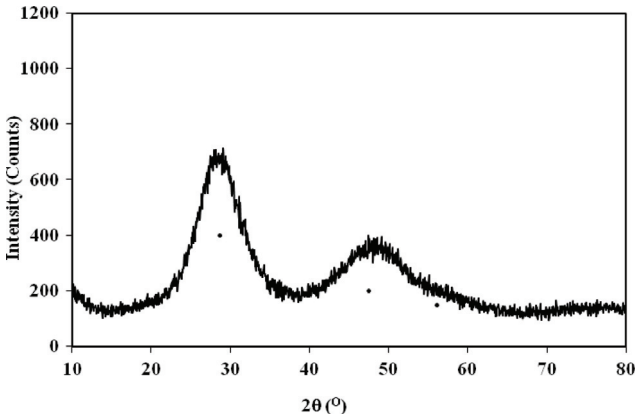

Fig. 2. XRD pattern of $Zn_{0.4}Cd_{0.6}S$ nanocomposite.

3.2. Degradation of dyes catalyzed by $Zn_XCd_{1-X}S$ nanocomposites

The photocatalytic effect of $Zn_XCd_{1-X}S$ nanocomposites (0.1 g/l) on degradation efficiency of CR within 20 min and MO, MR and MB within 60 min with initial concentration of 10 mg/l at pH 7 were indicated in Fig. 4. As seen, $Zn_{0.4}Cd_{0.6}S$ show the highest photocatalytic effect and thus the highest photodegradation efficiency was observed in the presence of $Zn_{0.4}Cd_{0.6}S$ as photocatalyst. ZnS and CdS as semiconductors have band-gap energy of 3.54 and 2.42 eV at 300 K, respectively. Apparently, the band-gap of nanocomposite is decreased with increasing the mole fraction of Cd in $Zn_XCd_{1-X}S$. As the band-gap gets narrower, the absorption spectrum moves into visible light range [3]. Thus, the production of electrons and holes are increased in conductance and valance bands, respectively, under simulated sunlight irradiation. The band-gap position of the $Zn_XCd_{1-X}S$ solid solutions can be adjusted by changing the ratio of the composition of CdS to that of ZnS. Generally, the more negative potential of the conduction band of the $Zn_XCd_{1-X}S$ solid solution shows the more photocatalytic activity. However, the photoreactivity of nanocomposites with

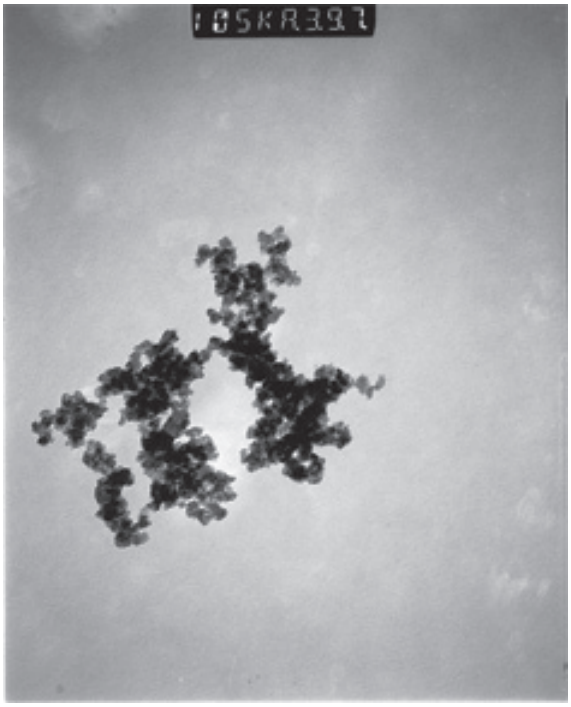

Fig. 3. TEM image of $Zn_{0.4}Cd_{0.6}S$ nanocomposite.

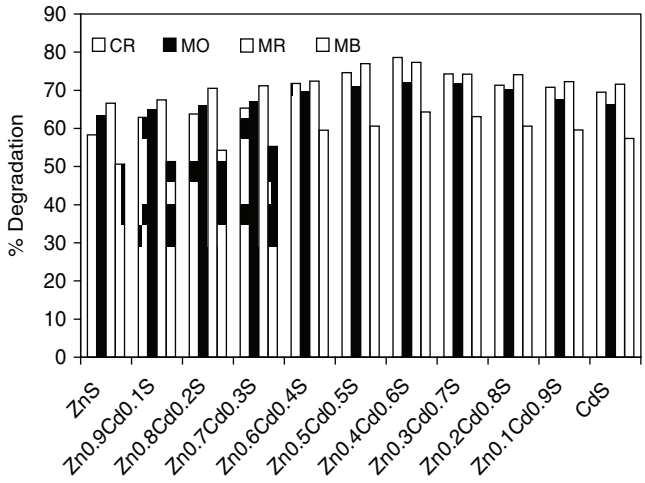

Fig. 4. Degradation efficiency of CR within 20 min and MO, MR and MB within 60 min.

X values of 0.3–0.5 is very similar because the band-gap and the surface morphology of these solid solutions are nearest together [2]. The CdS semiconductor with band-gap 2.42 eV show a recombination of the charge carries within surface states. Thus, a decreasing of photocatalytic activity was seen with increasing the mole fraction of Cd ($X_{Cd} > 0.6$) in $Zn_XCd_{1-X}S$ nanocomposites. Because, decreasing of band-gap is due to increasing probability of recombination of electrons and holes [22,23].

3.3. Optimization of photodegradation process

The parameters such as sample pH and dosage of photocatalyst influence on the degradation efficiency of a pollutant. The surface charge of catalyst and the charge of pollutant molecules are dependent pH [24]. As a consequence, the sample pH influence on the adsorption of pollutant molecules on the catalyst surface. The effect of pH on the photodegradation of dyes catalyzed by $Zn_{0.4}Cd_{0.6}S$ was studied in pH range of 2–12. The studies were performed at initial concentration 10 mg/l of dye and 0.1 g/l of catalyst. The pH of sample solutions was adjusted with adding of suitable amounts of HCl and NaOH with concentrations of 1.0×10^{-1} M. The results are shown in Fig. 5 within 20 min for CR and 60 min for MO, MR and MB.

As seen from Fig. 5, the highest degradation was obtained at pH 3 for MO and MR. While, the degradation of 78% was observed for CR at pH 5–7 and 80% for MB at pH 11. The isoelectric point (IEP) of ZnS and CdS was observed at pH 7–7.5 [25]. Therefore, it is expected that the IEP of $Zn_{0.4}Cd_{0.6}S$ composite, also, is occurred at pH 7.0–7.5. Thus, the surface charge of catalyst is positive in pH < 7 and negative in pH > 7.5. On the other hand, the charge of dye molecule is also different in various pHs because the functional groups.

Fig. 6 shows the degradation efficiency of dyes in different amounts of $Zn_{0.4}Cd_{0.6}S$ nanocomposite at range 0.1–0.7 g/l. The results indicate the increasing of degradation with increasing the amount of photocatalyst from 0.1 to 0.5 g/l and then diminish with loading of photocatalyst above of 0.5 g/l. The increasing of the decolorization rate may be due to the enhancement in the availability of active sites and thus the increasing of the number of dye

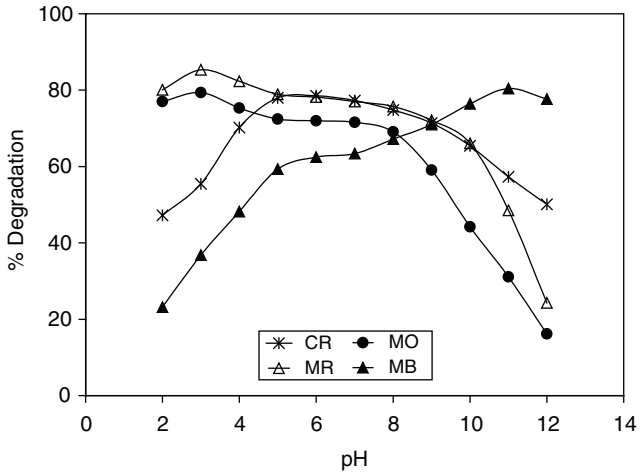

Fig. 5. The effect of sample pH on the degradation efficiency of dyes catalyzed by $Zn_{0.4}Cd_{0.6}S$ nanocomposite within 20 min for CR and 60 min for MO, MR and MB.

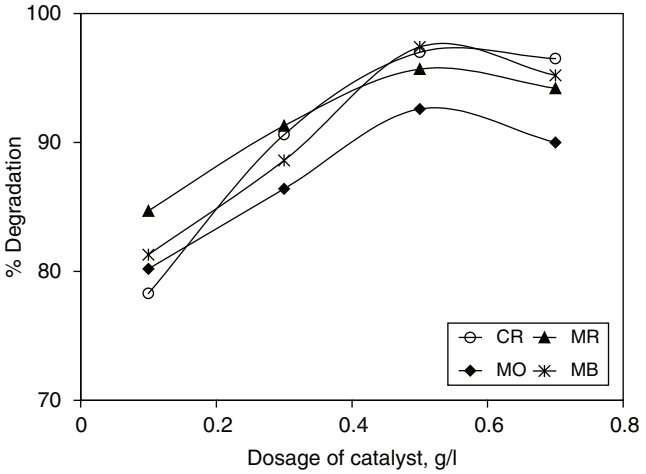

Fig. 6. Degradation efficiency of dyes (10 mg/l) catalyzed by $Zn_{0.4}Cd_{0.6}S$ composite in dosage of 0.1–0.7 g/l.

molecules adsorbed on the surface of catalyst as well as the increasing the density of particles in the area of illumination. At higher catalyst loading of 0.5 g/l, the degradation of dye decreases because the activated molecules are deactivated by agglomeration. The radiation penetration is decreased and the radiation scattering increase at higher amounts of photocatalyst [26,27].

Experiments were performed to study the effect of initial concentration of dyes in range of 10–50 mg/l on the rate of decolorization. The kinetic model for heterogeneous photocatalysis is in accordance with the Langmuir–Hinshelwood kinetic expression (Eqs. (3)–(5)) [28]

$$r = -\frac{d[\text{dye}]}{dt} = \frac{kK_{\text{dye}}[\text{dye}]}{1 + K_{\text{dye}}[\text{dye}]_0} = k_{\text{obs}}[\text{dye}] \quad (3)$$

$$r = \ln\frac{[\text{dye}]_0}{[\text{dye}]_t} = k_{\text{obs}}t \quad (4)$$

$$\frac{1}{k_{\text{obs}}} = \frac{1}{kK_{\text{dye}}} + \frac{[\text{dye}]_0}{k} \quad (5)$$

In Eqs. (3)–(5), $[\text{dye}]_0$ is the initial concentration of dye (mg/l), K_{dye} is the Langmuir–Hinshelwood adsorption equilibrium constant (l/mg), k is the rate constant of surface reaction (mg/l·min), and k_{obs} is the pseudo-first-order rate constant (min^{-1}). The obtained k_{obs}, K_{dye} and k values are shown in Table 2 and the kinetic curves of photodegradation reactions are indicated in Figs. 7–10. The rate of degradation of dyes was decreased with increasing the initial concentration. The decrease of degradation rate with enhancement the initial concentration of dye is due to two reasons: (i) increasing of

Table 2
The pseudo-first-order rate constants, k_{obs} (min^{-1}), of photocatalytic degradation at different initial concentration (C_0) of dyes, Langmuir–Hinshelwood adsorption equilibrium constant (K_{dye}, l/mg) and rate constant of surface reaction (k, mg/l·min)

Dye	C_0, mg/l					k	K_{dye}
	10	20	30	40	50		
CR	0.198	0.159	0.116	0.094	0.080	5.208	0.067
MO	0.043	0.036	0.030	0.025	0.022	1.767	0.033
MR	0.051	0.044	0.034	0.027	0.025	1.818	0.042
MB	0.065	0.047	0.039	0.030	0.026	1.718	0.062

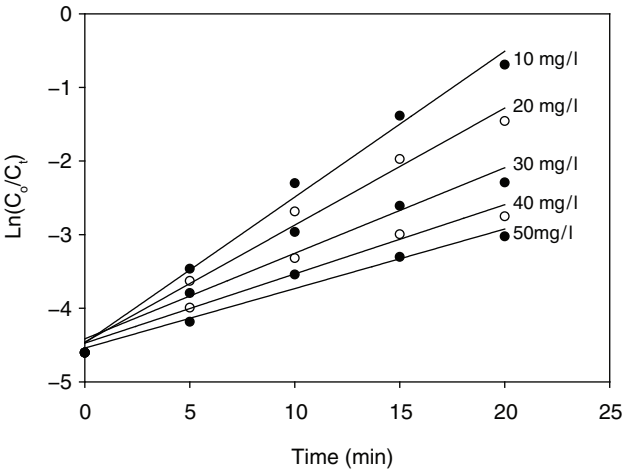

Fig. 7. Plot of $\text{Ln}(C_0/C_t)$ versus time at different initial concentration of CR (10.0–50.0 mg/l).

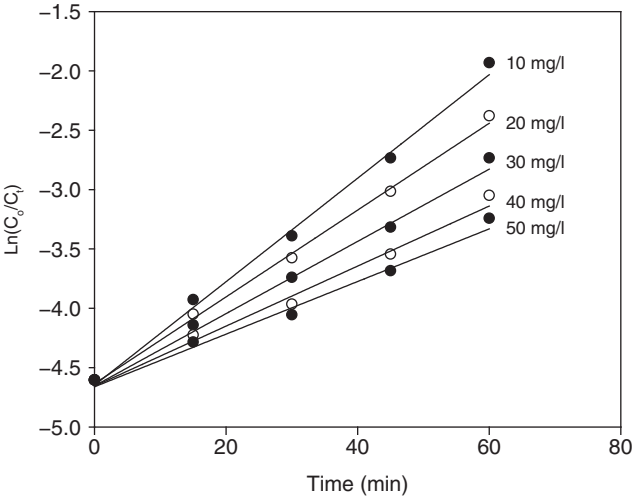

Fig. 8. Plot of $\text{Ln}(C_0/C_t)$ versus time at different initial concentration of MO (10.0–50.0 mg/l).

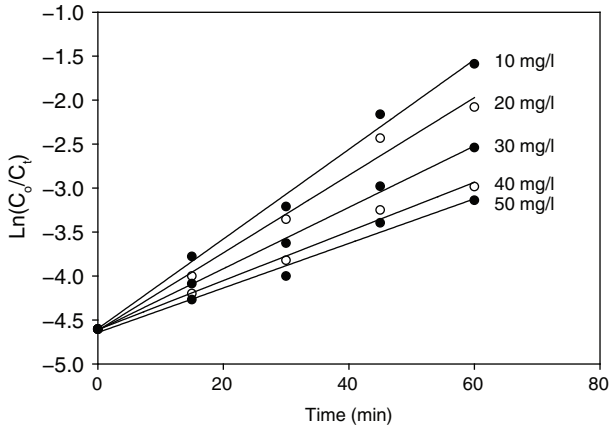

Fig. 9. Plot of $Ln(C_0/C_t)$ versus time at different initial concentration of MR (10.0–50.0 mg/l).

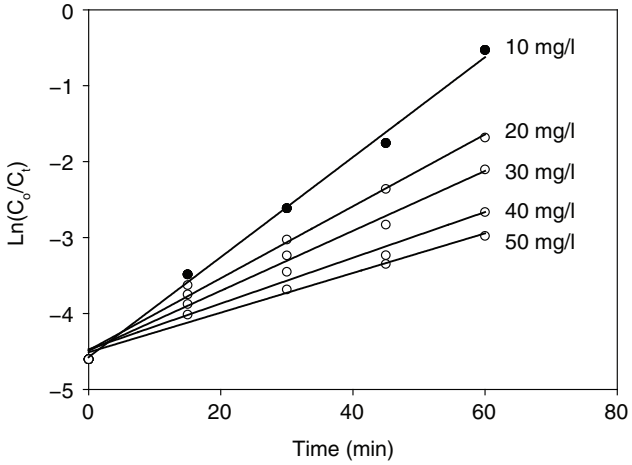

Fig. 10. Plot of $Ln(C_0/C_t)$ versus time at different initial concentration of MB (10.0–50.0 mg/l).

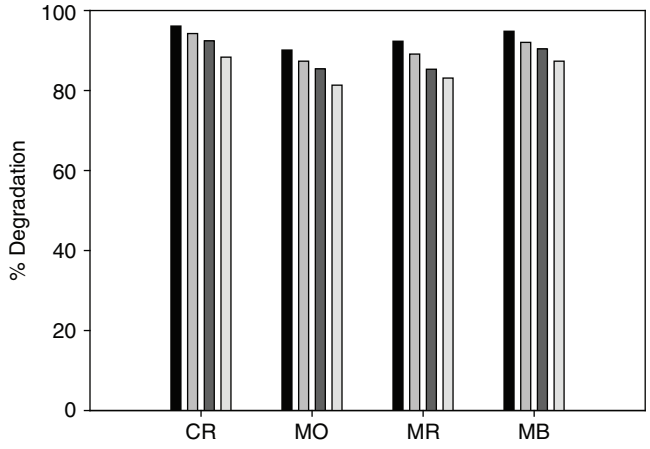

Fig. 11. Reusability of $Zn_{0.4}Cd_{0.6}S$ nanocomposite in photodegradation process of dyes in 4-cycles.

dye molecules adsorbed on the surface of the catalyst and decrease the active sites for generation of hydroxyl radicals at the catalyst surface, (ii) increasing the adsorb light by dye molecules and decrease the number of photons could reach the photocatalyst surface [29,30].

3.4. The reusability and photocorrosion of $Zn_{0.4}Cd_{0.6}S$ nanocomposite

The $Zn_{0.4}Cd_{0.6}S$ nanocomposite was used in 4-cycles under simulated sunlight irradiation. After each cycle, the nanocomposites are removed from sample, washed with water and ethanol and treated at 50°C in duration 2 h. The repeatability of photocatalytic activity of $Zn_{0.4}Cd_{0.6}S$ on the dye degradation is shown in Fig. 11.

The ideal photocatalyst should possess the properties such as photoactivity, biological and chemical inertness, stability toward photocorrosion, suitability towards visible or near UV light, low cost, and lack of toxicity [31]. The stability of $Zn_{0.4}Cd_{0.6}S$ nanocomposite was measured with determination of zinc and cadmium ions in irradiated sample with initial dosage of 0.5 g/l at pHs 3, 7 and 11. The results dissolution of nanocomposite are collected in Table 3. The negligible amounts of dissolution show the stability of nanocomposite toward photocorrosion in acidic, neutral and basic pHs.

3.5. Chemical oxygen demand

In addition to absorbance measurements for decolorization studies, it is necessary to analyze the degree of mineralization of the dyes to evaluate the degradation level applied under simulated sunlight irradiation using $Zn_{0.4}Cd_{0.6}S$ nanocomposite. COD values have been related to the total concentration of organic materials in the solution and the decrease of COD reflects the degree of mineralization. The mineralization efficiencies obtained after 20 min for CR and 60 min for MO, MR and MB are shown in Fig. 12. Also, the mineralization efficiency of a sample contains all of dyes after 120 min is indicated in Fig. 12. The maximum mineralization of 80% was obtained in CR degradation. The mineralization efficiency of 50% a sample contains dyes show the

Table 3

Dissolution of zinc and cadmium ions as weight percent (w/w%) in irradiated solution at different pHs

M^{2+}	pH		
	3	7	11
Zn^{2+}	0.29	0.04	0.21
Cd^{2+}	0.30	0.03	0.20

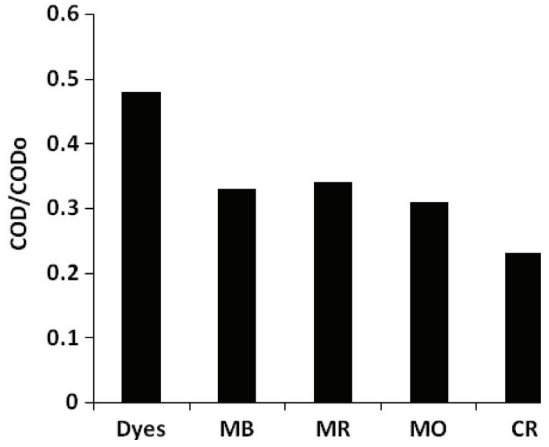

Fig. 12. The ratio of COD/COD_0 after 20 min for CR, 60 min for MO, MR and MB and 120 min of irradiation for a sample contain all of dyes.

photocatalyst activity of proposed nanocomposite. The COD value after irradiation indicates that there is still a residual amount of organic compounds, consisting of low mass molecules such as aldehydes and carboxylic acids in the treated solution [32]. It is noticed that the rate of decolorization is faster than the mineralization. As a result, the dyes do not oxidized completely into CO_2 and H_2O, because in most cases, reaction intermediates are formed in solution during the degradation of the dyes.

4. Conclusion

The coprecipitation method can be used to synthesis of $Zn_{0.4}Cd_{0.6}S$ nanocomposite. The $Zn_{0.4}Cd_{0.6}S$ nanocomposite show photocatalyst property in photodegradation process of dyes such as congo red, methyl orange, methyl red and methylene blue. The $Zn_{0.4}Cd_{0.6}S$ is not soluble in samples with pH of 3, 5 and 11. The proposed photocatalyst is reusable at least four times after treatment at 50°C. The mineralization of dyes was achieved at time less than 60 min with respect to the COD values.

References

[1] M. Ethayaraja, C. Ravikumar, D. Muthukumaran, K. Dutta and R. Bandyopadhyaya, CdS–ZnS core–shell nanoparticle formation: Experiment, mechanism, and simulation, J. Phys. Chem. C, 27 (2007) 3246–3252.
[2] C. Xing, Y. Zhang, W. Yan and L. Guo, Band structure-controlled solid solution of $Cd_{1-x}Zn_xS$ photocatalyst for hydrogen production by water splitting, Int. J. Hydrogen Energy, 31 (2006) 2018–2024.
[3] S. Zu, Z. Wang, B. Liu, X. Fan and G. Qian, Synthesis of nano-$Cd_xZn_{1-x}S$ by precipitate-hydrothermal method and its photocatalytic activities, J. Alloys Compds., 476 (2009) 689–692.
[4] Y. Nien, P. Chen and I. Chen, Synthesis and characterization of $Zn_{1-x}Cd_xS$:Cu, Cl red electroluminescent phosphor powders, J. Alloys Compds., 462 (2008) 398–403.
[5] S. Guha, B.J. Wu, H. Cheng and J.M. Depuydt, Microstructure and pseudomorphism in molecular beam epitaxially grown ZnCdS on GaAs(001), Appl. Phys. Lett., 63 (1993) 2129–2131.
[6] B.J. Wu, H. Cheng, S. Guha, M.A. Haase, J.M. Depuydt, G. Meishaugen and J. Qiu, Molecular beam epitaxial growth of CdZnS using elemental sources, Appl. Phys. Lett., 63 (1993) 2935–2937.
[7] J. Torres and G. Gordillo, Photoconductors based on $Zn_xCd_{1-x}S$ thin films, Thin Solid Films, 207 (1992) 231–235.
[8] D.L. Chen and L. Gao, Microemulsion-mediated synthesis of cadmium zinc sulfide nanocrystals with composition-modulated optical properties, Solid State Commun., 133 (2005) 145–150.
[9] Q.L. Nie, Q.L. Yuan, Q.S. Wang and Z.D. Xu, *In situ* synthesis of $Zn_xCd_{1-x}S$ nanorod by a hydrothermal route, J. Mater. Sci., 39 (2004) 5611–5612.
[10] K. Rajeshwar, M.E. Osugi, W. Chanmanee, C.R. Chenthamarakshan, M.V.B. Zanoni, P. Kajitvichyanukul and R. Krishnan-Ayer, Heterogeneous photocatalytic treatment of organic dyes in air and aqueous media, J. Photochem. Photobiol., C 9 (2008) 171–192.
[11] S.K. Kansal, M. Singh and D. Sudc, Studies on photodegradation of two commercial dyes in aqueous phase using different photocatalysts, J. Hazard. Mater., 141 (2007) 581–590.
[12] M.N. Rashed and A.A. El-Amin, Photocatalytic degradation of methyl orange in aqueous TiO_2 under different solar irradiation sources, Int. J. Phys. Sci., 2 (2007) 73–81.
[13] T. Aarthi, Prashanthi Narahari and Giridhar Madras, Photocatalytic degradation of Azure and Sudan dyes using nano TiO_2, J. Hazard. Mater., 149 (2007) 725–734.
[14] C. Namasivayam and D. Kavitha, Removal of congo red from water by adsorption onto activated carbon prepared from coir pith an agricultural solid waste, Dyes Pigments, 54 (2002) 47–58.
[15] Z. Aksu and S. Tezer, Equilibrium and kinetic modelling of biosorption of Remazol Black B by Rhizopus arrhizus in a batch system: effect of temperature, Process Biochem., 36 (2000) 431–439.
[16] M. Faisal, M. Abu Tariq and M. Muneer, Photocatalysed degradation of two selected dyes in UV-irradiated aqueous suspensions of titania, Dyes Pigments, 72 (2007) 233–239.
[17] L.F. Liotta, M. Gruttadauria, G. Di Carlo, G. Perrini and V. Librando, Heterogeneous catalytic degradation of phenolic substrates: Catalysts activity, J. Hazard. Mater., 162 (2009) 588–606.
[18] M.R. Hoffmann, Scot T. Martin, W. Choi and D.W. Bahnemannt, Environmental applications of semiconductor photocatalysis, Chem. Rev., 95 (1995) 69–96.
[19] S.D. Sartale, B.R. Sankapal, M. Lux-Steiner and A. Ennaoui, Preparation of nanocrystalline ZnS by a new chemical bath deposition route, Thin Solid Films, 480–481 (2005) 168–172.
[20] A. Guinier, X-ray Diffraction, San Francisco, CA, 1963.
[21] S. Brunauer, P.H. Emmett and E. Teller, Adsorption of gases in multimolecular layers, J. Am. Chem. Soc., 60 (1938) 309–319.
[22] P.V. Kamat and D. Meisel, Nanoparticles in advanced oxidation processes, Curr. Opin. Colloid Interface Sci., 7 (2002) 282–287.
[23] D. Beydoun, R. Amal, G. Low and S. McEvoy, Role of nanoparticles in photocatalysis, J. Nanopart. Res., 1 (1999) 439–458.
[24] G.R. Bamwenda, K. Sayama and H. Arakawa, The effect of selected reaction parameters on the photoproduction of oxygen and hydrogen from a WO_3–Fe^{2+}–Fe^{3+} aqueous suspension, J. Photochem. Photobiol., A 122 (1999) 175–183.
[25] H.R. Pouretedal, A. Norozi, M.H. Keshavarz and A. Semnani, Nanoparticles of zinc sulfide doped with manganese, nickel and copper as nanophotocatalyst in the degradation of organic dyes, J. Hazard. Mater., 162 (2009) 674–681.
[26] S. Hammami, N. Oturan, N. Bellekhal, M. Dachraoui and M.A. Oturan, Oxidative degradation of directorange 61 by electro-Fenton process using carbon felt electrode: application of the experimental design methodology, J. Electroanal. Chem., 610 (2007) 75–84.
[27] Q. Zhuo, H. Ma, B. Wang and F. Fan, Degradation of methylene blue: optimization of operating condition through a statistical technique and environmental estimate of the treated waste water, J. Hazard. Mater., 153 (2008) 44–51.

[28] H. Al-Ekabi and N. Serpone, Kinetic studies in heterogeneous photocatalysis, J. Phys. Chem., 92 (1988) 5726–5731.
[29] S. Senthilkumaar and K. Porkodi, Heterogeneous photocatalytic decomposition of crystal violet in UV-illuminated sol–gel derived nanocrystalline TiO_2 suspensions, J. Colloid Interface Sci., 288 (2005) 184–189.
[30] H.R. Pouretedal, H. Eskandari, M.H. Keshavarz and A. Semnani, Photodegradation of organic dyes using nanoparticles of cadmium sulfide doped with manganese, nickel and copper as nanophotocatalyst, Acta Chim. Slov., 56 (2009) 353–361.
[31] J. Suna, Y. Wang, R. Suna and S. Dong, Photodegradation of azo dye Congo Red from aqueous solution by the WO_3–TiO_2/activated carbon (AC) photocatalyst under the UV irradiation, Mater. Chem. Phys., 115 (2009) 303–308.
[32] S. Song, L. Xu, Z. He, H. Ying, J. Chen, X. Xiao and B. Yan, Photocatalytic degradation of C.I. Direct Red 23 in aqueous solutions under UV irradiation using $SrTiO_3$/CeO_2 composite as the catalyst, J. Hazard. Mater., 152 (2008) 1301–1308.